J. Plasma Phys. (2023), *vol*. 89, 965890301
Published by Cambridge University Press

doi:10.1017/S0022377823000491

Characteristics of betatron radiation in AWAKE Run 2 experiment

Linbo Liang[1,2], Hossein Saberi[1,2,†], Guoxing Xia[1,2,†], John Patrick Farmer[3,4] and Alexander Pukhov[5]

[1]Department of Physics and Astronomy, University of Manchester, Manchester M13 9PL, UK

[2]Cockcroft Institute, Daresbury, Cheshire WA4 4AD, UK

[3]CERN, 1211 Geneva, Switzerland

[4]Max Planck Institute for Physics, 80805 Munich, Germany

[5]Heinrich-Heine-Universität Düsseldorf, 40225 Düsseldorf, Germany

(Received 14 April 2023; revised 12 May 2023; accepted 22 May 2023)

The oscillating relativistic electrons in the accelerating/focusing wakefields of plasma accelerators emit electromagnetic radiation known as betatron radiation (BR). The proton-driven plasma wakefield acceleration has been demonstrated in the Advanced Wakefield Experiment (AWAKE) at CERN; however, its accompanying radiation emission is less explored compared with those in the laser- and electron beam-driven plasma accelerators. In this paper, a detailed simulation study of BR in the AWAKE is presented. Considering the new set-up of the AWAKE Run 2 (2021–), the radiation emission from both the witness electron beam and the seeding electron beam is investigated using particle-in-cell simulations. The influence of radial size mismatch and misaligned off-axis injection on the witness beam dynamics, as well as the spectral features of the relevant BR are studied. These non-ideal electron injections are likely to occur in experiment. The proton self-modulation stage is also investigated with a close look at the seeding electron beam dynamics and its BR. As a footprint of the emitting particles, BR can provide valuable information about the beam dynamics. Some practical challenges to implement the betatron diagnostic in the AWAKE Run 2 experiment are also addressed.

Key words: plasma simulation, plasma diagnostics, intense particle beams

1. Introduction

Plasma accelerators exhibit large longitudinally accelerating and transversely focusing fields in the wake behind the driver. In such intense fields, relativistic electrons oscillate while accelerating to higher energies and so emit synchrotron-like broadband radiation known as betatron radiation (BR) (Esarey *et al.* 2002; Wang *et al.* 2002; Kostyukov,

† Email addresses for correspondence: hossein.saberi@manchester.ac.uk; guoxing.xia@manchester.ac.uk

Kiselev & Pukhov 2003). In the past years, BR in laser- and electron beam-driven wakefield accelerators has been intensively investigated. In fact, with the advances of laser and plasma techniques, BR from laser wakefield accelerators has become a valuable short-pulse broadband X-ray source for imaging with high contrast (Kneip *et al.* 2010; Schnell *et al.* 2013). Betatron spectroscopy also works as a novel non-invasive beam diagnostic tool (Phuoc *et al.* 2006; Albert *et al.* 2008, 2013; Litos & Corde 2012; Corde *et al.* 2013*b*).

The Advanced Wakefield Experiment (AWAKE) is a proof-of-principle proton beam-driven plasma wakefield experiment at CERN. The AWAKE Run 1 experiment (2016–2018) has achieved the seeded self-modulation (SSM) of the proton bunch and the acceleration of externally injected 18.5 MeV electron beam up to 2 GeV (Adli *et al.* 2018). Following the success of Run 1, the AWAKE Run 2 experiment (2021–) aims to demonstrate the electron seeded proton self-modulation (eSSM), as well as to accelerate an externally injected electron bunch to multi-GeV energies, while preserving the beam emittance and energy spread (Muggli 2020). The Run 2 set-up will employ two successive 10 m-long plasma cells with a narrow gap in between. The first plasma cell and the 1 m gap are dedicated to eSSM and the relevant diagnostics, respectively. Moreover, a 150 MeV electron bunch following the modulated proton beam is also injected into the second plasma cell from the gap. The electron beam then is accelerated to higher energies via the proton-driven plasma wakefield. The AWAKE is installed upstream of the CNGS target area which is going to be dismantled. This allows a much longer (tens of metres) space for future set-up including the diagnostic instruments (Gschwendtner *et al.* 2022).

Betatron diagnostics for AWAKE Run 2 has been introduced in a previous work and a preliminary experimental set-up has been proposed (Williamson *et al.* 2020). In this paper, we systematically investigate the BR in AWAKE Run 2 for both the witness beam and the seeding electron beam. It is shown that possible non-ideal injection conditions of the witness electron beam, such as the beam radius mismatch and the transverse misalignment, can affect the beam dynamics and thus the spectral features of its BR. The beam dynamics and the radiation properties of the seeding electron bunch in the proton self-modulation stage is also studied.

This paper is organized as follows. The theoretical description of the BR in plasma ion column is presented in § 2. The beam dynamics and BR of the mismatched and misaligned off-axis injected witness electron bunch is discussed in § 3. The beam dynamics and the radiation from the low-energy seeding electron bunch are explored in § 4. The applicability of betatron diagnostics for the AWAKE is discussed in § 5 and some practical challenges are addressed. Conclusions are summarized in § 6.

2. Betatron radiation in plasma ion column

The plasma ion column driven by a laser pulse or particle bunch is a place where both intense longitudinal accelerating and transverse restoring forces co-exist (Kostyukov *et al.* 2003). The latter can cause betatron oscillations of off-axis electrons with the fundamental frequency of $\omega_\beta = \omega_p/\sqrt{2\gamma}$ and the wavelength of $\lambda_\beta = 2\pi c/\omega_\beta$. Here, γ is the Lorentz factor of the electron, c is the speed of light, $\omega_p = \sqrt{n_0 e^2/m_e\varepsilon_0}$ is the plasma frequency where e and m_e are the electron charge and mass, respectively, n_0 is the unperturbed plasma density, and ε_0 is the vacuum permittivity. The strength of the betatron oscillation is usually characterized by the normalized betatron oscillation amplitude K_β, which is defined as (Kostyukov *et al.* 2003)

$$K_\beta = \gamma k_\beta r_\beta = 1.33 \times 10^{-10}\sqrt{\gamma n_0\,[\mathrm{cm}^{-3}]}\, r_\beta[\mu\mathrm{m}], \tag{2.1}$$

https://doi.org/10.1017/S0022377823000491 Published online by Cambridge University Press

where $k_\beta = k_p/\sqrt{2\gamma}$ is the betatron wave number, $k_p = \omega_p/c$ is the plasma wave number and r_β is the betatron oscillation amplitude.

Depending on the strength of K_β, the BR is mainly categorized into two regimes. The limit of small amplitude near axis betatron oscillations with $K_\beta \ll 1$ is known as the undulator regime. The undulator radiation is narrowly peaked at the fundamental mode ($n = 1$) with a wavelength of $\lambda = \lambda_\beta/2\gamma^2$ (Esarey *et al.* 2002). However, if the betatron oscillation amplitude is large enough, i.e. $K_\beta \gg 1$, radiation from different sections of the electron's trajectory will be emitted in different directions, contributing to a wide opening angle $\Psi = K_\beta/\gamma$ of the radiation cone in the direction perpendicular to the electron oscillation plane. The radiation frequency range also gets wide as high harmonics with finite bandwidth become significant. This regime is known as the wiggler regime.

Finite variations of the plasma wiggler parameter K_β for different electrons in the bunch will broaden the bandwidth of each harmonic and lead to an overlap of different frequency spikes. So the betatron spectrum in the plasma ion column appears as a quasi-continuous broadband spectrum, similar to the synchrotron radiation from a bending dipole magnet. This synchrotron-like spectrum has been demonstrated experimentally in laser-plasma experiments (Rousse *et al.* 2004; Kneip *et al.* 2010; Fourmaux *et al.* 2011).

The asymptotic spectrum of the wiggler radiation of a single electron with constant energy is given by (Esarey *et al.* 2002)

$$S_{\gamma,r_\beta}(\omega, \Omega) \sim \frac{\gamma^2\zeta^2}{1+\gamma^2\theta^2}\left[\mathrm{K}^2_{2/3}(\zeta) + \frac{\gamma^2\theta^2}{1+\gamma^2\theta^2}\mathrm{K}^2_{1/3}(\zeta)\right], \tag{2.2}$$

where $\mathrm{K}_\nu(\zeta)$ is the modified Bessel function of the second kind, $\zeta = (\omega/\omega_c)(1+\gamma^2\theta)^{3/2}$, ω is the radiation frequency, θ is the deflection angle relative to the electron propagation direction and the critical photon frequency ω_c is defined as (Kostyukov *et al.* 2003)

$$\omega_c = \frac{2}{3}\gamma^3 c r_\beta k_\beta^2. \tag{2.3}$$

The critical photon frequency is meaningful since half of the radiation power is emitted above/below the frequency of ω_c. The radiation intensity falls exponentially and becomes negligible for frequencies beyond ω_c. The normalized photon energy spectrum is obtained by integrating (2.2) over all spatial angles (θ, ϕ), which has the shape of the universal function for the synchrotron-like emission

$$S_{\gamma,r_\beta}(\omega) = (\omega/\omega_c)\int_{\omega/\omega_c}^{\infty} \mathrm{K}_{5/3}(\omega/\omega_c)\,\mathrm{d}(\omega/\omega_c). \tag{2.4}$$

In plasma wakefield accelerators, the spatial scale of the electron bunch is typically of the order of ~μm, which is much larger than the betatron radiation wavelength (~nm). So the radiation spectrum of a bunch can be simplified as the incoherent summation of the single-electron spectrum (Esarey *et al.* 2002; Curcio *et al.* 2017*b*).

Numerical simulations are carried out by the three-dimensional (3-D) quasi-static particle-in-cell (PIC) code QV3D (Pukhov 2016), which is developed on the VLPL platform (Pukhov 1999). QV3D calculates the emission of each macroparticle analytically at each time step. The synchrotron radiation is calculated self-consistently from the transverse momentum change of the macroparticle in one time step. This change in momentum determines how many photons are emitted. The momentum of the macroparticle is then updated according to the energy loss to consider the influence of the radiation reaction. The output of the code is the integrated critical photon spectrum

https://doi.org/10.1017/S0022377823000491 Published online by Cambridge University Press

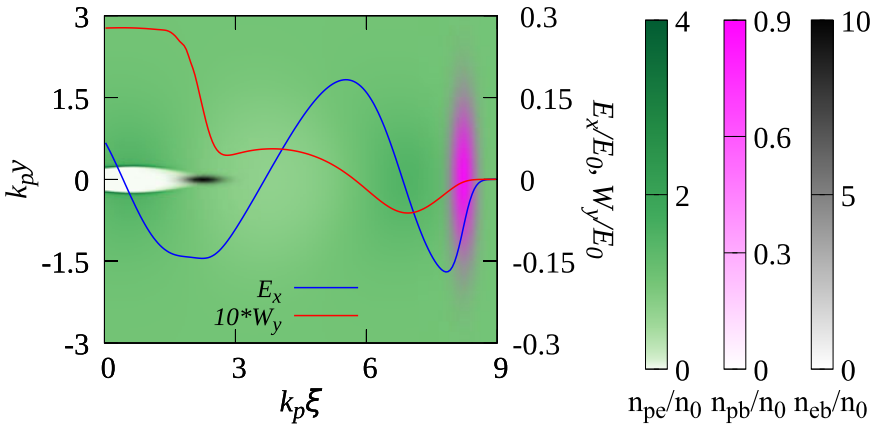

FIGURE 1. Schematic of simplified AWAKE Run 2 acceleration stage (Liang *et al.* 2022). The densities of plasma electrons (n_{pe}, green), the proton driver (n_{pb}, magenta) and the witness electron bunch (n_{eb}, black) are shown in contour plots. Particle beams propagate from left to right. Here, $\xi = x - ct$ is the longitudinal coordinate in the co-moving frame. The blue solid line represents the loaded longitudinal wakefield E_x, and the red dashed line is the transverse wakefield $W_y = E_y - cB_z$ at the transverse position of σ_{ic}.

per spatial angle, and so the betatron spectrum should be reconstructed by a convolution with the universal function as shown in (2.4).

3. Radiation from the witness electron bunch

For the AWAKE Run 2, the proton self-modulation and the electron acceleration stages are separated into two different plasma cells. The electron-seeded self-modulated proton beam from the first plasma cell is injected into the second plasma cell to drive the acceleration wakefield. The witness electron beam with an energy of 150 MeV is injected in the wakefield right after the proton microbunches. It then accelerates along 10 m plasma aiming at high-quality high-energy electron beam.

A full PIC modelling of the proton dynamics combining with the electron acceleration will be very expensive in time and computer resources. The relativistic proton bunch is quite rigid (with heavy mass and relatively large gamma factor), so the proton bunch after the self-modulation does not change significantly (Adli *et al.* 2019). Therefore, for simplicity, the acceleration scheme is described by a toy model that was first introduced by Olsen, Adli & Muggli (2018). The model consists of a single highly rigid proton bunch as the driver and a trailing witness electron bunch in the background plasma as shown in figure 1 (Liang *et al.* 2022). The driver particle mass is magnified by 10^{10} times on the base of the real proton mass in the simulation. Since such a dummy proton bunch is highly rigid, the proton-driven wakefield also remains static in its own frame during the propagation except for the dephasing with respect to the witness bunch. This model allows to focus on the acceleration physics of the witness electron beam.

Necessary particle beams and plasma parameters for simulations are presented in table 1. Parameters of the non-evolving driver bunch are set to simulate the quasi-linear wakefield excited by the self-modulated SPS proton bunch train (Olsen *et al.* 2018). The simulation window co-moving with the particle bunches at the speed of light has the dimension of $(9 \times 6 \times 6)k_p^{-1}$ and resolution of $(0.05 \times 0.01 \times 0.01)k_p^{-1}$ in directions of (x, y, z), where x is the longitudinal direction, and y and z are transverse directions. The

https://doi.org/10.1017/S0022377823000491 Published online by Cambridge University Press

	Symbol	Value	Unit
Rubidium plasma			
Density	n_0	7×10^{14}	cm^{-3}
Proton driver			
Energy	E_{p0}	400	GeV
Lorentz factor	γ_{p0}	426	
Charge	Q_p	2.34	nC
r.m.s. Bunch length	$\sigma_{\xi p}$	40	μm
r.m.s. Bunch radius	σ_{rp}	200	μm
Electron witness			
Energy	E_{e0}	150	MeV
Lorentz factor	γ_{e0}	294	
Energy spread	$\Delta\gamma/\gamma_{e0}$	0.1 %	
Charge	Q_e	120	pC
r.m.s. Bunch length	$\sigma_{\xi e}$	60	μm
Normalized emittance	ε_{n0}	6.84	μm

TABLE 1. The AWAKE baseline parameters for simulation.

simulation time step is chosen as $5\omega_p^{-1}$, which is short enough to resolve the envelope evolution of the witness bunch. The number of macroparticles per cell is four for the plasma with fixed ion background and one for the non-evolving proton driver. The witness beam is simulated with 10^6 equally weighted macroparticles.

The waist of the witness bunch should match to the pure plasma ion background at the entrance of the plasma column to prevent beam envelope or root-mean-square (r.m.s.) beam radius oscillation. The matched radial size for a Gaussian beam in the plasma ion column is defined by (Olsen *et al.* 2018; Litos *et al.* 2019)

$$\sigma_{ic} = \left(\frac{2\epsilon_{n0}^2}{\gamma_{e0} k_p^2} \right)^{1/4}, \tag{3.1}$$

where $\epsilon_{n0} = \beta_{e0}\gamma_{e0}\epsilon_0$ is the normalized r.m.s. beam emittance, ϵ_0 is the initial geometric emittance, and γ_{e0} and $\beta_{e0} = \sqrt{1 - 1/\gamma_{e0}^2}$ are the initial mean Lorentz factor and the normalized velocity of the witness beam, respectively. Equation (3.1) gives a matched beam size of $\sigma_{ic} = 10.64$ μm for the parameters in table 1, which results in a normalized peak bunch density of $n_{e0}/n_0 \approx 10$ for a Gaussian profile bunch. Since the witness bunch is dense enough, it can further blow out the plasma electrons forming a plasma bubble with linear radial focusing force. The longitudinal wakefield excited by the witness bunch also loads upon the proton-driven wakefield, resulting in a relatively uniform net accelerating gradient along the bunch. The initial delay between the two bunches is fixed to $k_p\Delta\xi = 6$ for all cases presented in this work.

The non-ideal conditions are highly likely to happen in the experiment, leading to unexpected results. For instance, during electron beam injection into the plasma, the ideal conditions of the matched radius and the on-axis injection may break down. In the following, these non-ideal cases and their influence on the electron beam dynamics and the relevant radiation emission are explored.

https://doi.org/10.1017/S0022377823000491 Published online by Cambridge University Press

3.1. *Influence of mismatched beam radius*

In experiment, it is always difficult to precisely match the electron beam to the pure ion channel due to the various errors in the beam transport, e.g. the jitters in the magnetic field, the misalignment of magnets, etc. Additionally, the plasma bubble with longitudinally uniform focusing strength covers only the rear part of the witness beam, while at its head, the plasma focusing strength varies with the sinusoidal quasilinear plasma wave, thereby the matching conditions are not entirely identical for different slices along the witness beam. With different extent of mismatch radius along the beam, the witness beam undergoes a fast and intense envelope expansion and oscillation after being injected into the plasma, especially at the bunch head. This leads to a rapid emittance growth at the initial period of beam propagation until full phase-mixing (Liang *et al.*, 2022; Farmer *et al.* 2022). Nevertheless, it is shown that the mismatch of the whole bunch's r.m.s. radius does not necessarily lead to the further degradation of the beam quality. There is actually a wide mismatch tolerance depending on the beam charge and length (Farmer *et al.* 2022).

Figure 2(*a*) shows the evolution trends of the r.m.s. beam radius during the acceleration process for five cases with different initial beam radii. For $\sigma_r/\sigma_{ic} < 1$, the bubble formation is much quicker at the beginning. However, the witness bunch is over dense so the emittance pressure (emittance induced defocusing force) exceeds the plasma focusing force. This leads to a rapid expansion of the beam envelope along the whole bunch in the first few tens of centimetres. The transverse expansion of the bunch size is mostly pronounced at the bunch head, because the transverse focusing force in the quasi-linear wake is much weaker than in the bubble. In such cases, the r.m.s. beam radius of the whole bunch after 10 m is larger than the 'matched' case. The reduction of the bunch radius with respect to the maximum value is due to the adiabatic damping effect, with the scaling law of $\sigma_r \propto \gamma^{-1/4}$. For $\sigma_r/\sigma_{ic} > 1$, the aforementioned physical process is reversed for the rear part of the beam in the plasma bubble. However, for its head part, there is an 'optimal' (quasi-matched) initial r.m.s. radius in the range of $1.25 \leq \sigma_{r0}/\sigma_{ic} \leq 1.5$. Below these values, the radius of the head part first sees an expansion before the adiabatic damping. When the initial beam radius exceeds these 'optimal' values, the emittance pressure is lower than the plasma focusing force along the bunch, so the entire bunch remains focused during the whole process of acceleration. The large initial bunch radius results in a smaller r.m.s. beam radius quickly, thus a larger average bunch density is obtained. This causes the overloading of the proton-driven wakefield, which then leads to a lower average acceleration gradient. As a consequence, the final energy gain is lower for cases with larger initial bunch radii, as shown in figure 2(*b*). However, since the variation of the quasi-uniform acceleration gradient due to the mismatch and adiabatic damping effects is relatively small, the difference of the final energy gain for different mismatched cases is also small. The average energy gain, therefore, increases quasi-linearly during the acceleration.

Figure 3(*a*) shows the betatron photon energy spectra of the witness electron bunch with different initial bunch radii. The difference is almost negligible for all cases. This is possibly because these betatron spectra are the results of the emission integrated over multiple betatron oscillations up to the diagnostic point at $s = 10$ m. To quantitatively characterize the betatron photon spectra, we can estimate the critical photon energy via the relation (Esarey *et al.* 2002)

$$\hbar\omega_c = \hbar \langle\omega\rangle \,/\, \left(8/15\sqrt{3}\right), \tag{3.2}$$

where $\hbar \langle\omega\rangle$ is the mean photon energy. Figure 3(*b*) shows the total number of photons N emitted during the acceleration which is almost linearly increasing during the beam

https://doi.org/10.1017/S0022377823000491 Published online by Cambridge University Press

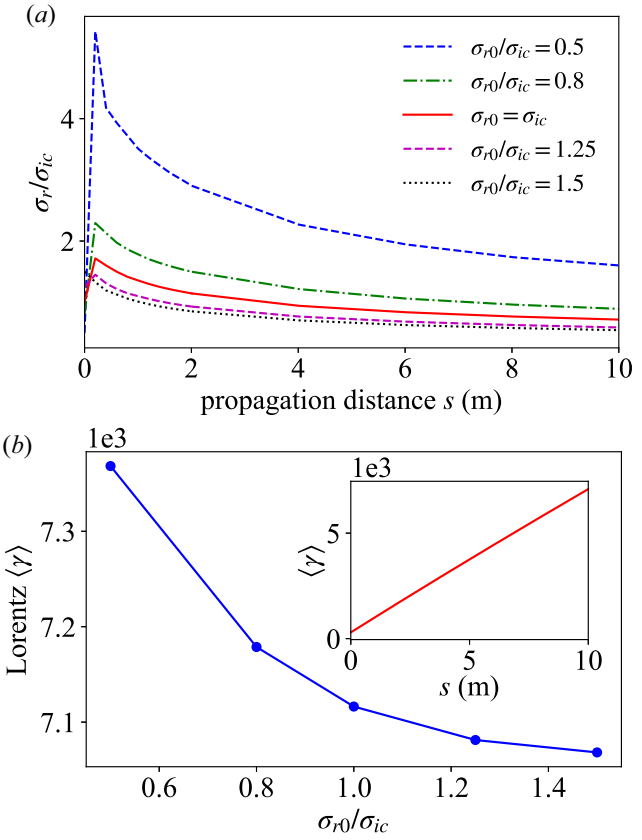

FIGURE 2. (*a*) Normalized r.m.s. beam radius σ_r/σ_{ic} versus the acceleration distance s. (*b*) Dependency of the average Lorentz factor $\langle\gamma\rangle$ on the normalized initial beam radius σ_{r0}/σ_{ic}, measured after 10 m propagation in plasma. The inset shows the evolution of $\langle\gamma\rangle$ for the matched case during the beam acceleration.

propagation. Prior research has suggested that the total photon emission of a single electron scales as $N \propto N_\beta K_\beta$ for the wiggler regime and $N \propto N_\beta K_\beta^2$ for the undulator regime where N_β is the number of oscillations (Esarey *et al.* 2002; Corde *et al.* 2013*a*). To illustrate the relative change of the betatron emission, lineouts showing the dependencies of the critical photon energy on the initial bunch radius are plotted in figure 3(*c*). The critical photon energies are normalized by the value of the matched case. At the early moments, e.g. $s = 0.4$ m, the critical photon energy is nearly proportional to the initial beam radius. During the acceleration, the relative difference of $\hbar\omega_c$ for different cases gets smaller due to the larger contribution of the high energy photon emission near the plasma exit. One can also notice that the critical photon energy of the cases with smaller radii exceeds that of the matched one after $s = 8$ m. This is likely due to the over expansion of the bunch head which results in the betatron oscillations with larger amplitudes.

To reconstruct the beam profile and emittance, the spatial distribution of its emission is needed (Curcio *et al.* 2017*a*). So it is interesting to look at the spatial distribution of betatron photons. The radiation pattern on the screen is axisymmetric for an axisymmetric electron bunch (Kostyukov *et al.* 2003); therefore, we look at the angular photon distribution with respect to the axial angle θ. The angle θ represents the ratio between

https://doi.org/10.1017/S0022377823000491 Published online by Cambridge University Press

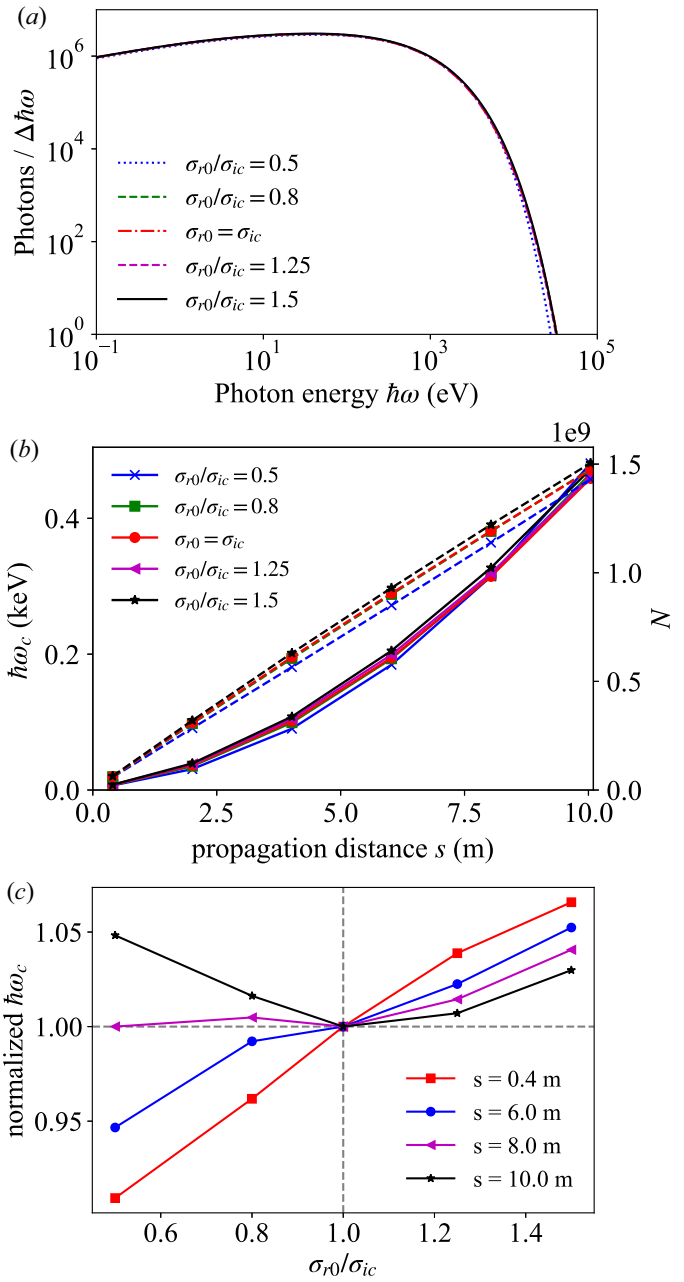

FIGURE 3. (*a*) Photon energy spectrum measured at $s = 10$ m. Here, $\Delta\hbar\omega$ is 10^{-3} of the photon energy measuring range, given by the horizontal axis. (*b*) Evolution of the critical photon energy $\hbar\omega_c$ (solid lines) and the total number of emitted photons N (dashed lines) along the acceleration distance s. (*c*) Normalized critical photon energy $\hbar\omega_c$ with respect to the value of matched case versus the normalized initial beam radius σ_{r0}/σ_{ic}.

the radial position r_s of betatron photons on a virtual screen and the distance L_s between the screen and the plasma entrance, i.e. $\theta \approx r_s/L_s$, as illustrated in figure 4(*a*). It shows that the betatron photons are confined within a narrow axial angle, with the r.m.s. value

https://doi.org/10.1017/S0022377823000491 Published online by Cambridge University Press

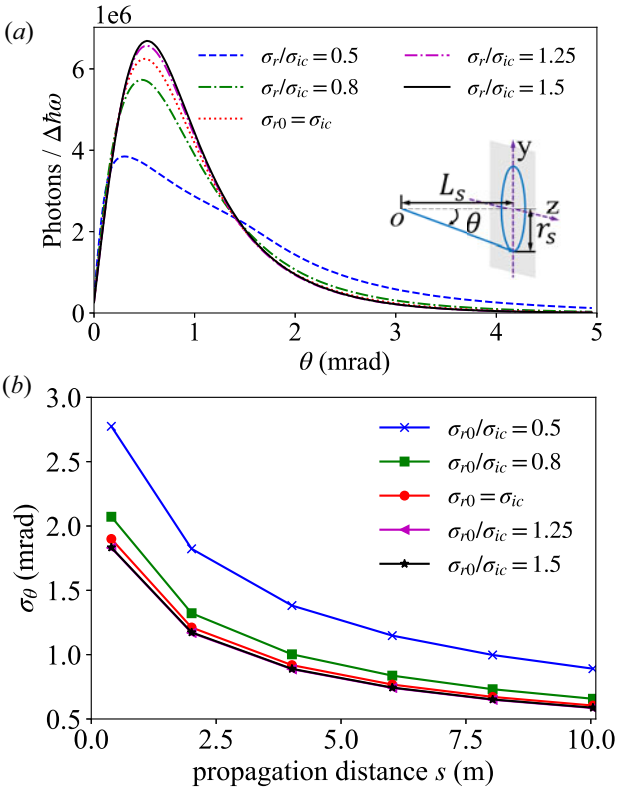

FIGURE 4. (*a*) Photon angular distribution versus the axial angle θ measured at $s = 2$ m. (*b*) Evolution of the r.m.s. value of θ versus the acceleration distance s.

of $\sigma_\theta = (1/N \sum_i \theta_i^2)^{1/2} < 2$ mrad for photons measured at $s = 2$ m. The photon angular distribution shapes have good agreement with the transverse distributions of the witness beam in different cases. Furthermore, we can see that the evolution trend of σ_θ in figure 4(*b*) is similar to that of the r.m.s. beam radius in figure 2(*a*).

3.2. *Influence of misaligned off-axis electron injection*

In § 3.1, the witness electron bunch is injected on the central axis of the wakefield for ideal acceleration. The on-axis injected electron bunch does not suffer from the possible transverse instabilities like hosing (Huang *et al.* 2007). This instability can be induced by the off-axis or oblique electron injection and cause a large increase of the beam emittance and even lead to the beam breakup (BBU) if the instability becomes strong enough. Therefore, understanding the influence of misaligned off-axis electron beam injection on the beam dynamics and the corresponding radiation emission would be useful for AWAKE.

The focusing force and therefore the betatron oscillation depend on the transverse position of electrons, so it is expected that the off-axis injection leads to stronger betatron emission with higher photon energy. The polarization of BR can also be enhanced in the preferred oscillation direction, i.e. the offset direction of the bunch (Kostyukov *et al.* 2003). This is due to the fact that the transverse focusing force in the axisymmetric wakefield is pointing towards the axis of the wake structure.

https://doi.org/10.1017/S0022377823000491 Published online by Cambridge University Press

Here we look at several cases in which the witness bunch has minor offsets from the axis: $\Delta r_0/\sigma_{ic} = 0$, 0.35, 0.71 and 1, where $\Delta r_0 = \sqrt{\Delta y_0^2 + \Delta z_0^2}$ is the combined initial offset of the transverse beam centroid, and Δy_0 and Δz_0 are the initial offsets in the y- and z-directions, respectively. For the second and third cases, the beam offsets are only in the y-direction. For the last one, equal offsets of $0.71\sigma_{ic}$ in both y- and z-directions are considered, which correspond to a combined offset of $\Delta r_0 = \sigma_{ic}$ along the azimuthal angle $\phi = \pi/4$ in the y–z plane. These minor offsets allow to investigate the BR from the witness bunch without significant charge loss due to the transverse instabilities. Additionally, similar cases with a higher charge of 400 pC are also studied. Higher charge can compensate the beam emittance growth induced by the minor offset at the injection point, as the bubble formation is much quicker for the high charge bunch (Farmer *et al.* 2022).

Figure 5 shows that when the radial offset is larger than $0.71\sigma_{ic}$, the beam radiates with higher critical photon energy than the on-axis injection. For smaller offsets, the amplification in photon energy is not significant. Similar trends can also be found in the radiation of the 400 pC witness bunch. This may suggest a safe range for driver-witness misalignment at the injection point. In figure 5(*a*), one can also see that the 400 pC bunch can produce more BR than the baseline, which is mainly due to more charge contributing to the radiation process. Additionally, figure 5(*b*) shows that the critical photon energies of cases with 400 pC charge are generally lower than the baseline, which is essentially due to the lower average accelerating wakefields after beam loading.

Figure 6 shows the 2-D photon angular distribution over the two spatial angles θ and ϕ, and the 1-D projection on the azimuthal angle ϕ. As expected, the enhancement of the radiation occurs in the direction of the initial offset, e.g. $\phi = \pi/4$ and $-3\pi/4$ for the offsets of $+0.71\sigma_{ic}$ in both y- and z-directions as shown in figure 6(*a*). We also notice that the off-axis injection reshapes the photon density distribution with respect to the axial angle θ. In the offset direction, the photons fall in a wide range of the angle θ, while in other directions, the betatron photons are confined radially within a much narrower θ angle (Claveria *et al.* 2019). Prior works have shown that for an electron oscillating in a plane along the propagation direction, the typical opening angle of the radiation cone scales as $\Theta \sim K_\beta/\gamma$ in the trajectory plane, while in the vertical direction, it scales as $\Theta \sim 1/\gamma$ (Wang *et al.* 2002; Rousse *et al.* 2004). In figure 6(*b*), we can find that the enhancement of the radiation along the initial offset direction leads to the reduction of photon emission at other angles of ϕ, compared with the on-axis injection. This enhancement is also stronger for cases with higher charge. This feature may allow us to deduce the beam misalignment direction via the betatron diagnostics at the plasma exit.

4. Radiation from the seeding electron bunch

In the first plasma cell of the AWAKE Run 2 experiment, an electron bunch seeds the proton self-modulation when it runs ahead of the long proton bunch (Muggli *et al.* 2020). The electron seeded self-modulation will offer better control on the wakefield's phase and amplitude than the self-modulation growing from random noise. In this section, simulations are performed to study the seeding electron beam dynamics and its relevant betatron spectrum features. Parameters are generally similar to that used in the preliminary electron seeding experiment (Verra *et al.* 2022). The electron beam has an initial energy of 18.5 MeV, charge of 250 pC, radial size of $\sigma_{r0} = 0.2$ mm and duration of $\sigma_t = 5$ ps ~ 1.5 mm. The plasma density is $n_0 = 2 \times 10^{14}$ cm^{-3}. Other simulation environment settings are similar to those in the previous section.

Some of the main bunch statistics, such as the r.m.s. radial size σ_r, total normalized beam energy W/W_0 and the relative energy spread $\Delta\gamma/\langle\gamma\rangle$, are shown in figure 7.

https://doi.org/10.1017/S0022377823000491 Published online by Cambridge University Press

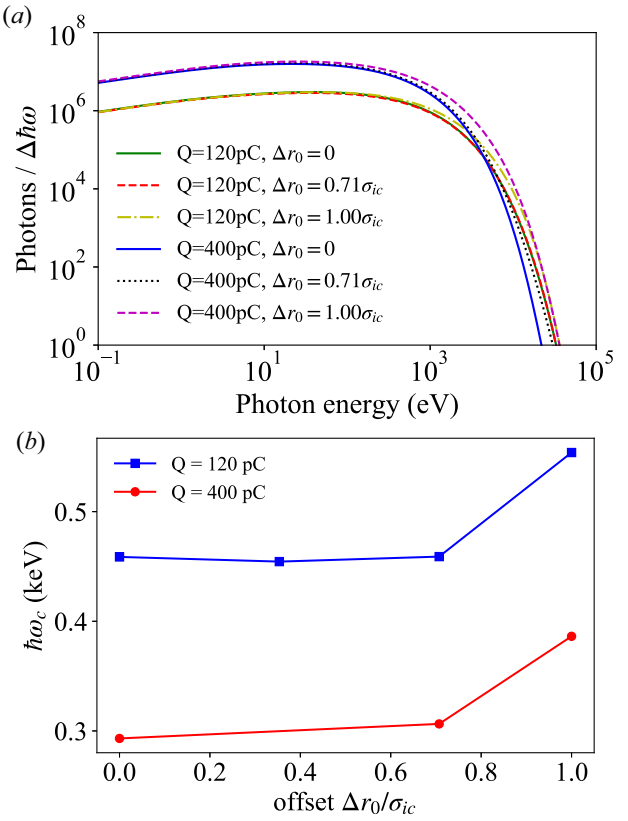

FIGURE 5. (*a*) Betatron photon energy spectrum at $s = 10$ m for different injection offsets. Both the baseline witness beam and higher charge beam (400 pC) are considered. (*b*) Corresponding critical photon energies versus the beam offsets.

The fast increase of the radial r.m.s. beam size σ_r in the first 0.5 m is due to the defocusing of seeding electrons at the head and the tail of the bunch where the local plasma focusing force is too weak to compensate the emittance-induced defocusing effect. This results in approximately 25 % charge leaving the simulation window without significant deceleration. After that, the remaining electrons get focused by its wakefield which leads to the reduction of the beam size, and hence the increase of the seed wakefield amplitude. These electrons are widely distributed over decelerating and accelerating phases after $s = 1$ m, which leads to a huge increase of the beam energy spread, but no significant net deceleration. The energy of electrons at the bunch head is quickly depleted in the plasma after approximately 5 m, so they start to slip backwards into the defocusing phase, which results in a significant bunch size expansion and charge loss. As a result of this second-stage charge loss, the remaining electron bunch is cooled down as shown by the decrease of the energy spread. The overall beam energy also sees a larger decrease.

Figure 8 shows the betatron photon energy spectra and the photon angular distributions of the seeding electron beam. The integrated spectra are measured over different locations along the plasma cell. It can be seen that the photon energy spectra and the corresponding angular distributions do not evolve too much during the beam propagation. Calculation shows that the critical photon energy of the seeding beam radiation is decreasing in this process, but the change is less than 10 % for critical energy at $s = 1$ m (12.9 meV) and

https://doi.org/10.1017/S0022377823000491 Published online by Cambridge University Press

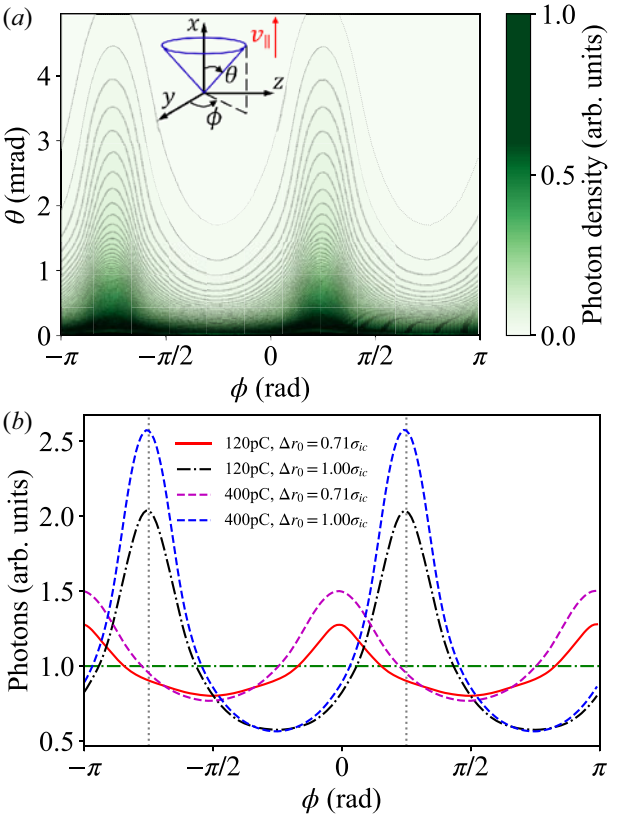

FIGURE 6. (*a*) Two-dimensional photon angular distribution of the baseline witness bunch with offsets of $0.71\sigma_{ic}$ in both y- and z-directions. The inset shows the spherical coordinates used to represent the photon spatial distribution. (*b*) The 1-D dependencies of photon numbers on the azimuthal angle ϕ. Here, $\phi = 0$ and $\pm\pi$ represents the $\pm y$ directions, respectively, and $\pm\pi/2$ are the $\pm z$ directions. The photon densities are normalized by the value of the on-axis injection for both the 120 pC and 400 pC beams. The azimuthal distribution of the on-axis injection is represented by the horizontal green dash–dotted line.

$s = 10$ m (11.7 meV). Similarly, the r.m.s. angle σ_θ also slightly decreases from 4.2 mrad (at $s = 1$ m) to 3.8 mrad (at $s = 10$ m). In fact, the increasing contribution of the low energy photon emission at a latter time from a larger portion of focused electrons oscillating in low amplitudes leads to the decrease of the critical photon energy and the r.m.s. angle. However, the maximum photon energy sees a small increase which probably is because of the presence of a fraction of accelerated and defocused electrons.

5. Discussion

The results of the paper are important for future AWAKE diagnostics design and understanding the beam dynamics inside the plasma. The correlation between BR and the electron dynamics has shown that we may possibly use BR to indirectly get information about the evolution of the electron beam. However, as shown by this work and the previous study (Williamson *et al.* 2020), there are several difficulties in the application of betatron diagnostics for the AWAKE.

https://doi.org/10.1017/S0022377823000491 Published online by Cambridge University Press

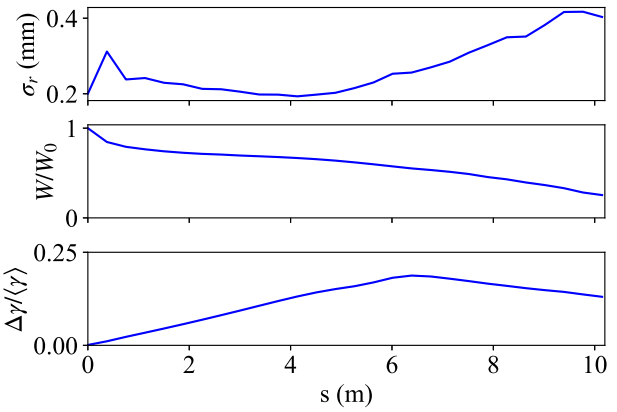

FIGURE 7. Evolution of the seeding electron bunch with respect to its propagation distance s in the plasma. Here, σ_r is the r.m.s. beam radius, $W = Q\langle\gamma\rangle$ is the total energy stored in the bunch, where Q and $\langle\gamma\rangle$ are the charge and the mean Lorentz factor, and $\Delta\gamma/\langle\gamma\rangle$ is the relative energy spread.

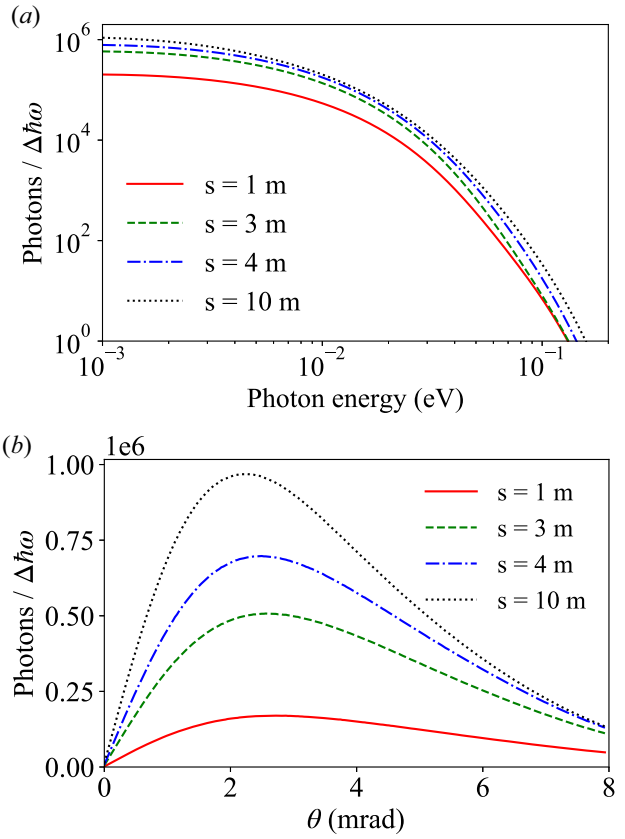

FIGURE 8. (*a*) Integrated BR spectra measured over different locations in the plasma. (*b*) Corresponding 1-D photon angular distributions with respect to the angle θ.

https://doi.org/10.1017/S0022377823000491 Published online by Cambridge University Press

The main problem from the physical side is the witness beam evolution due to its acceleration, which then changes the characteristics of the BR emitted at each moment along the acceleration path. The betatron photons emitted from different electrons and at different times/positions are accumulated on the screen of the spectrometer; therefore, the integrated radiation spectrum will be detected. However, as demonstrated in this paper, integrated BR can reveal some features of the beam, specially to distinguish non-ideal experimental electron beam injections like electron beam mismatch and the misaligned off-axis injection.

As the (modulated-) proton bunch coexists with electron bunches in both stages, it is also interesting to look at the radiation from the proton bunch. The main difficulty for the simulation study of the proton bunch radiation is the huge simulation cost due to the relatively large scale of the problem (e.g. the SPS proton beam length is 6 cm). Instead, we can give an estimation of the typical betatron photon energy radiated by a single proton via (2.3). This calculation gives an upper limit of the betatron photon energy. For a 400 GeV proton oscillating at an initial radial position of $\sigma_{rp} = 0.2$ mm in the plasma ion column of low (2×10^{14} cm^{-3}) and high (7×10^{14} cm^{-3}) densities, the critical photon energy is $E_c = 89$ meV and $E_c = 313$ meV, respectively. Since this photon energy is almost in the same range of the seeding electron bunch radiation, it may therefore be difficult to distinguish the BR from the two kinds of particles in the first plasma cell (modulation stage). However, at the acceleration stage where the electron radiation energy, typically in VUV to X-ray range, is much higher than that of the protons, this would not be a problem for witness beam betatron spectroscopy. In other words, one can use a filter and a specific VUV/X-ray camera to select the radiation from the witness electrons only.

Another possible source of interference for betatron spectroscopy could be the low-energy photons emitted by oscillating background plasma electrons (Kostyukov *et al.* 2003). This part of radiation mainly originates from the oscillations of low energy plasma electrons in the quasi-linear wakefields. The acceleration of plasma electrons due to the self-injection in the nonlinear regime (Kostyukov *et al.* 2009) is unlikely to happen in the AWAKE Run 2. Therefore, the interference from the background plasma electron radiation is negligible.

The practical application of the betatron diagnostics for the seeding beam in the first plasma cell is very challenging with the current technology because of: (i) the highly evolving electron beam at different phases, i.e. acceleration/deceleration and focusing/defocusing; (ii) the small gap between the plasma cells (approximately 1 m), and the high energy rigid proton beam, and (iii) the radiation at almost the same energy range from both the seeding beam and the proton beam. It should be noticed that the emission from the seeding beam will not be an issue for betatron spectroscopy of the witness beam, because of the completely different range of frequencies.

In the current experiment set-up, the witness electron beam is deflected by the electron spectrometer after a few metres from the exit of plasma cell, while the proton beam moves almost straight to the beam dump. The betatron spectroscopy of the witness beam radiation is possible as long as the energetic rigid proton beam does not damage the detection tools. This is possible by using a mirror with a hole in the centre to allow a proton bunch to go through, as suggested by Williamson *et al.* (2020). It is worth mentioning that the CNGS target area where the AWAKE is installed, is going to be dismantled. This allows tens of metres space for the future set-up including the diagnostic instruments (Gschwendtner *et al.* 2022). Therefore, rather than the preliminary experimental proposal (Williamson *et al.* 2020), a full collection of emitted photons might be possible in the future by slightly deflecting the proton beam away from the central axis where the photons propagate.

https://doi.org/10.1017/S0022377823000491 Published online by Cambridge University Press

6. Conclusion

The AWAKE Run 2 experiment employs two successive plasma cells to separate the proton self-modulation and the electron acceleration stages. The seeding electron beam in the first plasma cell and the witness electron beam in the second one are the main sources of betatron emission. In this article, we studied the BR from both electron bunches in the AWAKE Run 2. The simulation results show that the BR can reveal the evolution of the witness electron beam properties, such as the r.m.s. radial size and average beam energy. In addition, BR of the witness beam can also identify non-ideal cases such as the radial bunch size mismatch and offset of the witness electron bunch at the injection point. This may work as a useful feedback for the injection system. Moreover, we examined the radiation from the seeding electron bunch in the self-modulation stage. Our work provides a further understanding of the BR properties in the AWAKE Run 2 and contributes to the study of betatron diagnostics for future proton-driven wakefield accelerators.

Acknowledgements

Editor V. Malka thanks the referees for their advice in evaluating this article.

Funding

This work was supported by the Cockcroft Institute (core grant number ST/V001612/1); and the STFC (AWAKE Run 2 grant numbers ST/T001917/1, ST/X00614X/1).

Declaration of interests

The authors report no conflict of interest.

REFERENCES

ADLI, E., AHUJA, A., APSIMON, O., APSIMON, R., BACHMANN, A.-M., BARRIENTOS, D., BARROS, M.M., BATKIEWICZ, J., BATSCH, F., BAUCHE, J., *et al.* 2019 Experimental observation of proton bunch modulation in a plasma at varying plasma densities. *Phys. Rev. Lett.* **122**, 054802.

ADLI, E., AHUJA, A., APSIMON, O., APSIMON, R., BACHMANN, A.-M., BARRIENTOS, D., BATSCH, F., BAUCHE, J., BERGLYD OLSEN, V.K., BERNARDINI, M., *et al.* 2018 Acceleration of electrons in the plasma wakefield of a proton bunch. *Nature* **561**, 363–367.

ALBERT, F., POLLOCK, B.B., SHAW, J.L., MARSH, K.A., RALPH, J.E., CHEN, Y.-H., ALESSI, D., PAK, A., CLAYTON, C.E., GLENZER, S.H., *et al.* 2013 Angular dependence of betatron X-ray spectra from a laser-wakefield accelerator. *Phys. Rev. Lett.* **111**, 235004.

ALBERT, F., SHAH, R., PHUOC, K.T., FITOUR, R., BURGY, F., ROUSSEAU, J.-P., TAFZI, A., DOUILLET, D., LEFROU, T. & ROUSSE, A. 2008 Betatron oscillations of electrons accelerated in laser wakefields characterized by spectral x-ray analysis. *Phys. Rev.* E **77**, 056402.

CLAVERIA, P.S.M., ADLI, E., AMORIM, L.D., AN, W., CLAYTON, C.E., CORDE, S., GESSNER, S., HOGAN, M.J., JOSHI, C., KONONENKO, O., *et al.* 2019 Betatron radiation andemittance growth in plasmawakefield accelerators. *Phil. Trans. R. Soc.* A **377**, 20180173.

CORDE, S., TA PHUOC, K., LAMBERT, G., FITOUR, R., MALKA, V., ROUSSE, A., BECK, A. & LEFEBVRE, E. 2013*a* Femtosecond x rays from laser-plasma accelerators. *Rev. Mod. Phys.* **85**, 1–48.

CORDE, S., THAURY, C., LIFSCHITZ, A., LAMBERT, G., TA PHUOC, K., DAVOINE, X., LEHE, R., DOUILLET, D., ROUSSE, A. & MALKA, V. 2013*b* Observation of longitudinal and transverse self-injections in laser-plasma accelerators. *Nat. Commun.* **4** (1), 1501.

CURCIO, A., ANANIA, M., BISESTO, F., CHIADRONI, E., CIANCHI, A., FERRARIO, M., FILIPPI, F., GIULIETTI, D., MAROCCHINO, A., MIRA, F., *et al.* 2017*a* Single-shot non-intercepting profile monitor of plasma-accelerated electron beams with nanometric resolution. *Appl. Phys. Lett.* **111** (13), 133105.

CURCIO, A., ANANIA, M., BISESTO, F., CHIADRONI, E., CIANCHI, A., FERRARIO, M., FILIPPI, F., GIULIETTI, D., MAROCCHINO, A., PETRARCA, M., *et al.* 2017*b* Trace-space reconstruction of

low-emittance electron beams through betatron radiation in laser-plasma accelerators. *Phys. Rev. Accel. Beams* **20**, 012801.

Esarey, E., Shadwick, B.A., Catravas, P. & Leemans, W.P. 2002 Synchrotron radiation from electron beams in plasma-focusing channels. *Phys. Rev.* E **65**, 056505.

Farmer, J., Liang, L., Ramjiawan, R., Velotti, F., Weidl, M., Gschwendtner, E. & Muggli, P. 2022 Injection tolerances for AWAKE Run 2c. arXiv:2203.11622.

Fourmaux, S., Corde, S., Phuoc, K.T., Leguay, P.M., Payeur, S., Lassonde, P., Gnedyuk, S., Lebrun, G., Fourment, C., Malka, V., *et al.* 2011 Demonstration of the synchrotron-type spectrum of laser-produced betatron radiation. *New J. Phys*. **13** (3), 033017.

Gschwendtner, E., Lotov, K., Muggli, P., Wing, M., Agnello, R., Ahdida, C.C., Amoedo Goncalves, M.C., Andrebe, Y., Apsimon, O., Apsimon, R, *et al.* 2022 The awake run 2 programme and beyond. *Symmetry* **14**, 1680.

Huang, C., Lu, W., Zhou, M., Clayton, C.E., Joshi, C., Mori, W.B., Muggli, P., Deng, S., Oz, E., Katsouleas, T., *et al.* 2007 Hosing instability in the blow-out regime for plasma-wakefield acceleration. *Phys. Rev. Lett*. **99**, 255001.

Kneip, S., McGuffey, C., Martins, J.L., Martins, S.F., Bellei, C., Chvykov, V., Dollar, F., Fonseca, R., Huntington, C., Kalintchenko, G., *et al.* 2010 Bright spatially coherent synchrotron x-rays from a table-top source. *Nat. Phys*. **6** (12), 980–983.

Kostyukov, I., Kiselev, S. & Pukhov, A. 2003 X-ray generation in an ion channel. *Phys. Plasmas* **10** (12), 4818–4828.

Kostyukov, I., Nerush, E., Pukhov, A. & Seredov, V. 2009 Electron self-injection in multidimensional relativistic-plasma wake fields. *Phys. Rev. Lett*. **103**, 175003.

Liang, L., Xia, G., Pukhov, A. & Farmer, J.P. 2022 Acceleration of an electron bunch with a non-Gaussian transverse profile in proton-driven plasma wakefield. *Appl. Sci*. **12**, 10919.

Litos, M. & Corde, S. 2012 Betatron radiation from a beam driven plasma source. *AIP Conf. Proc*. **1507** (1), 705–710.

Litos, M.D., Ariniello, R., Doss, C.E., Hunt-Stone, K. & Cary, J.R. 2019 Beam emittance preservation using gaussian density ramps in a beam-driven plasma wakefield accelerator. *Phil. Trans. R. Soc.* A **377** (2151), 20180181.

Muggli, P. 2020 Physics to plan AWAKE Run 2. *J. Phys.: Conf. Ser*. **1596** (1), 012008.

Muggli, P., Guzman, P.I.M., Bachmann, A.-M., Hüther, M., Moreira, M., Turner, M. & Vieira, J. 2020 Seeding self-modulation of a long proton bunch with a short electron bunch. *J. Phys.: Conf. Ser*. **1596** (1), 012066.

Olsen, V.K.B., Adli, E. & Muggli, P. 2018 Emittance preservation of an electron beam in a loaded quasilinear plasma wakefield. *Phys. Rev. Accel. Beams* **21**, 011301.

Phuoc, K.T., Corde, S., Shah, R., Albert, F., Fitour, R., Rousseau, J.-P., Burgy, F., Mercier, B. & Rousse, A. 2006 Imaging electron trajectories in a laser-wakefield cavity using betatron x-ray radiation. *Phys. Rev. Lett*. **97**, 225002.

Pukhov, A. 1999 Three-dimensional electromagnetic relativistic particle-in-cell code VLPL (Virtual Laser Plasma Lab). *J. Plasma Phys*. **61** (3), 425–433.

Pukhov, A. 2016 Particle-In-Cell codes for plasma-based particle acceleration. In *Proceedings of the 2014 CAS-CERN Accelerator School: Plasma Wake Acceleration, Geneva, Switzerland, 23–29 November 2014* (ed. B. Holzer). CERN, CERN-2016-001.

Rousse, A., Phuoc, K.T., Shah, R., Pukhov, A., Lefebvre, E., Malka, V., Kiselev, S., Burgy, F., Rousseau, J.-P., Umstadter, D., *et al.* 2004 Production of a kev x-ray beam from synchrotron radiation in relativistic laser-plasma interaction. *Phys. Rev. Lett*. **93**, 135005.

Schnell, M., Sävert, A., Uschmann, I., Reuter, M., Nicolai, M., Kämpfer, T., Landgraf, B., Jäckel, O., Jansen, O., Pukhov, A., *et al.* 2013 Optical control of hard x-ray polarization by electron injection in a laser wakefield accelerator. *Nat. Commun*. **4** (1), 2421.

Verra, L., Zevi Della Porta, G., Pucek, J., Nechaeva, T., Wyler, S., Bergamaschi, M., Senes, E., Guran, E., Moody, J.T., Kedves, M.A., *et al.* 2022 Controlled growth of the self-modulation of a relativistic proton bunch in plasma. *Phys. Rev. Lett*. **129**, 024802.

https://doi.org/10.1017/S0022377823000491 Published online by Cambridge University Press

WANG, S., CLAYTON, C.E., BLUE, B.E., DODD, E.S., MARSH, K.A., MORI, W.B., JOSHI, C., LEE, S., MUGGLI, P., KATSOULEAS, T., *et al.* 2002 X-ray emission from betatron motion in a plasma wiggler. *Phys. Rev. Lett*. **88**, 135004.

WILLIAMSON, B., XIA, G., GESSNER, S., PETRENKO, A., FARMER, J. & PUKHOV, A. 2020 Betatron radiation diagnostics for AWAKE Run 2. *Nucl. Instrum. Meth. Phys. Res.* A **971**, 164076.

https://doi.org/10.1017/S0022377823000491 Published online by Cambridge University Press